Fatigue Damaging Micromechanisms in Ductile Cast Irons

M. Cavallini[1], O. Di Bartolomeo[2], F. Iacoviello[2]

[1] Università di Roma La Sapienza, I.C.M.M.P.M., via Eudossiana 18, Roma, Italy
[2] Università di Cassino, Di.M.S.A.T., via G. Di Biasio 43, 03043 Cassino (FR), Italy, iacoviello@unicas.it

ABSTRACT. *Ductile iron discovery in 1948 gave a new lease on life to the cast iron family. In fact these cast irons are characterised both by a high castability and by high toughness values, combining cast irons and steel good properties. Ductile cast irons are also characterised by high fatigue crack propagation resistance, although this property is still not widely investigated.*
In the present work we considered three different ferritic-pearlitic ductile cast irons, characterised by different ferrite/pearlite volume fractions, and an austempered ductile cast iron. Their fatigue crack propagation resistance was investigated in air by means of fatigue crack propagation tests according to ASTM E647 standard, considering three different stress ratios ($R = K_{min}/K_{max} = 0.1; 0.5; 0.75$). Crack surfaces were extensively analysed by means of a scanning electron microscope both considering a traditional procedure and performing a quantitative analysis of 3D reconstructed surfaces, mainly focusing graphite nodules debonding mechanisms and considering the microstructure influence.

INTRODUCTION

In 1943, in the International Nickel Company Research Laboratory, a magnesium addition allowed to obtain a cast iron containing not flakes but nearly perfect graphite spheres. In 1948, a small amount of cerium allowed to obtain the same result. As a consequence of these chemical composition modifications, a very interesting combination of overall properties was obtained: high ductility (up to more than 18%), high strength (up to 850 MPa and, considering austempered ductile iron, up to 1600 MPa) and good wear resistance. Ductile irons were born. They are widely used in a number of applications, e.g. wheels, gears, crankshafts in cars and trucks etc.

Matrix controls these good mechanical properties and matrix names are used to designate spheroidal cast iron types. Ferritic ductile irons are characterised by good ductility and a tensile strength that are equivalent to a low carbon steel. Pearlitic ductile irons show high strength, good wear resistance and moderate ductility. Ferritic-pearlitic grades properties are intermediate between ferritic and pearlitic ones. Martensitic ductile irons show very high strength, but low levels of toughness and ductility. Bainitic grades are characterised by a high hardness. Austenitic ductile irons show good corrosion resistance, good strength and dimensional stability at high temperature. Austempered grades show a very high wear resistance and fatigue strength [1, 2].

The fatigue crack propagation resistance has been found to be dependent on the microstructure, the size and the volume fraction of graphite, graphite elements shape and the chemical composition [3]. Graphite spheroids increase the importance of crack closure effect, with a strong microstructure influence [4]. SEM fracture surface analysis and crack path profile analysis allowed to qualitatively identify the microstructure influence on graphite spheroids debonding.

In this work, four different ductile irons were considered (three ferritic-pearlitic and an austempered ductile irons) and their fatigue crack resistance was investigated. Fracture surface was investigated by SEM and a quantitative analysis of 3D reconstructed surfaces was performed, mainly focusing graphite nodules debonding mechanisms and considering the microstructure influence.

MATERIALS AND EXPERIMENTAL METHODS

Four ductile irons with different microstructures were considered with the chemical compositions reported on tables 1-4.

Table 1. Ductile iron EN GJS350-22 chemical composition (100% ferrite)

C	Si	Mn	S	P	Cu	Cr	Mg	Sn
3.66	2.72	0.18	0.013	0.021	0.022	0.028	0.043	0.010

Table 2. Ductile iron EN GJS500-7 chemical composition (50% ferrite – 50% pearlite)

C	Si	Mn	S	P	Cu	Cr	Mg	Sn
3.65	2.72	0.18	0.010	0.03	-	0.05	0.055	0.035

Table 3. Ductile iron EN GJS700-2 chemical composition (5% ferrite – 95% pearlite)

C	Si	Mn	S	P	Cu	Mo	Ni	Cr	Mg	Sn
3.59	2.65	0.19	0.012	0.028	0.04	0.004	0.029	0.061	0.060	0.098

Table 4. Austempered ductile iron GGG 70BA chemical composition (fully bainitic)

C	Si	Mn	Mo	Ni	Sn	S
3,61	2,23	0,32	0,42	0,52	0,045	0,015

Investigated ferritic-pearlitic ductile irons are characterized by a very high nodularity of graphite elements (Fig. 1). This implies that graphite elements could be considered as perfect spheres embedded in a metal matrix.

After the austempering treatment, austempered ductile iron is characterized by a reduced graphite spheroids degeneration and a good homogeneity of bainitic microstructure is obtained, with some residual ferrite around graphite elements (Fig. 2). In this case, graphite elements could be only roughly be approximated with spheres. This will be considered during the results discussion.

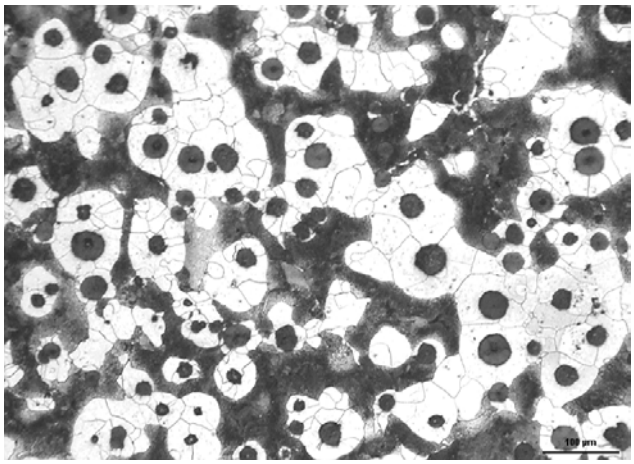

Figure 1. Ferritic-pearlitic ductile iron microstructure (Nital 3)

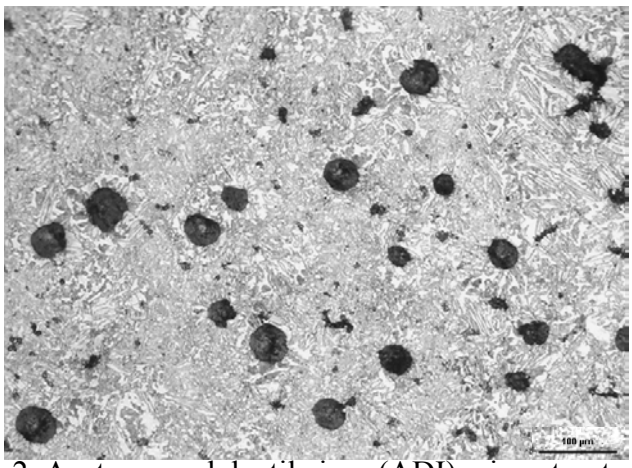

Figure 2. Austempered ductile iron (ADI) microstructure (Nital 3).

Fatigue tests were run according to ASTM E647 standard [5], using CT (Compact Type) 10 mm thick specimens and considering three different stress ratio values (e.g. $R = P_{min}/P_{max} = 0.1; 0.5; 0.75$). Tests were performed using a computer controlled INSTRON 8501 servohydraulic machine in constant load amplitude conditions, considering a 20 Hz loading frequency, a sinusoidal waveform and laboratory conditions. Crack length measurements were performed by means of a compliance

method using a double cantilever mouth gage and controlled using an optical microscope (x40). Fracture surfaces were analysed by means of a Philips scanning electron microscope (SEM). Furthermore, a 3D fracture surface reconstruction procedure was followed, in order to obtain a quantitatively reconstructed fracture surface and to perform a quantitative analysis of the microstructure influence on the graphite elements debonding mechanism [4]. Corresponding to the same specimen position, a stereoscopic image is obtained performing an eucentric tilting around the vertical axis and capturing two different images, with a tilting angle equal to 5° (tilting results in a static center point in the image). 3D surface reconstruction was performed using the Alicona MeX software and allowed to obtain images as in Fig. 3. Fracture surface profiles were quantitatively investigated as reported in Fig. 4.

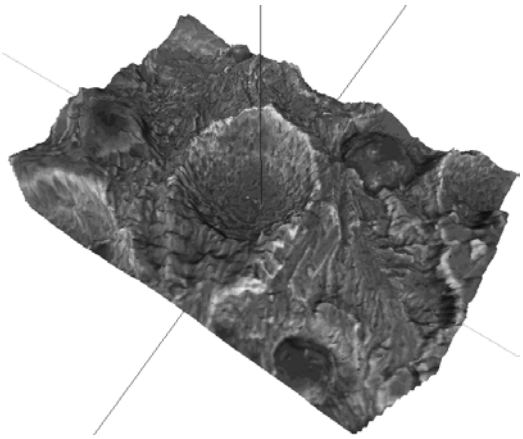

Figure 3. 3D reconstructed fracture surface (50% ferrite – 50% pearlite)

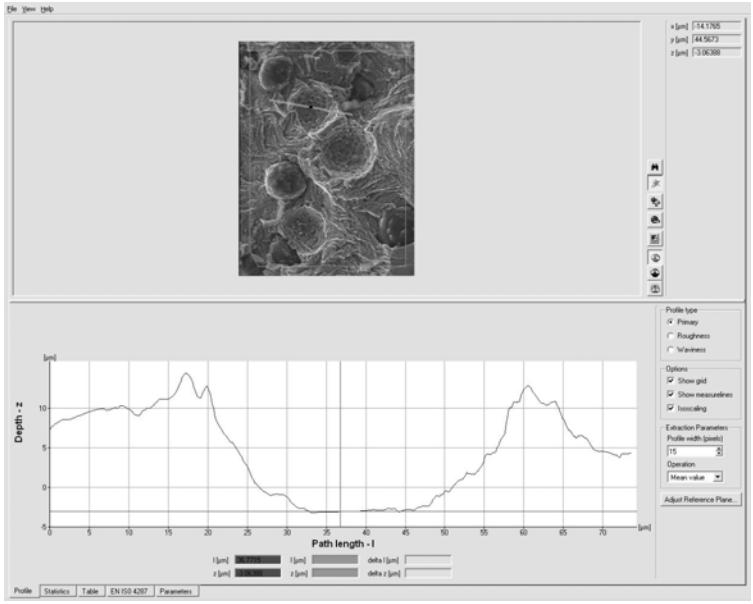

Figure 4. Fracture surface profile quantitative analysis.

At least 50 voids were investigated for all the considered ductile irons. Each void was characterized considering an approximation sphere and its geometry, and three different geometrical parameters were considered:

- Void depth "K" [μm];
- Void diameter "L" [μm];
- Approximation sphere diameter "D" [μm]

Relations among these geometric parameters depend on debonding process. If graphite elements debonding is completely fragile, it follows that $K \leq D/2$ and $L \leq D/2$. On the other side, a ductile debonding process implies $K > D/2$ and $L > D/2$, with differences that increase with the importance of ductile damage mechanism.

RESULTS

Stress ratio and microstructure influence on fatigue crack propagation are shown in figure 5. For R = 0.1, microstructure influence is almost negligeable. The increase of the stress ratio implies an increase of the microstructure influence, with the ferritic-pearlitic (50%-50%) and the austempered ductile iron that are characterized by lower crack growth rates for the same applied ΔK values, in stages II and III (Paris stage and final rupture stage), and higher final rupture values. Lower ΔK values are not clearly influenced by microstructure, and they decrease with the increase of the stress ratio for the same crack growth rate.

SEM fracture surface "traditional" analysis (Fig. 6) shows differences due to the different microstructures [4, 6, 7].

Graphite elements debonding results to be a common damaging mechanism characterized by a morphology that depend on the microstructure and relationships between the voids morphology parameters mentioned above are shown in Figs. 7 and 8.

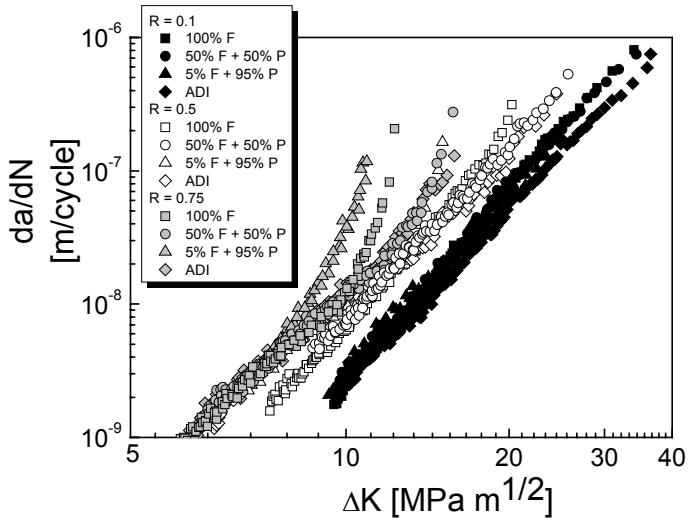

Figure 5: Microstructure and stress ratio influence on fatigue crack propagation.

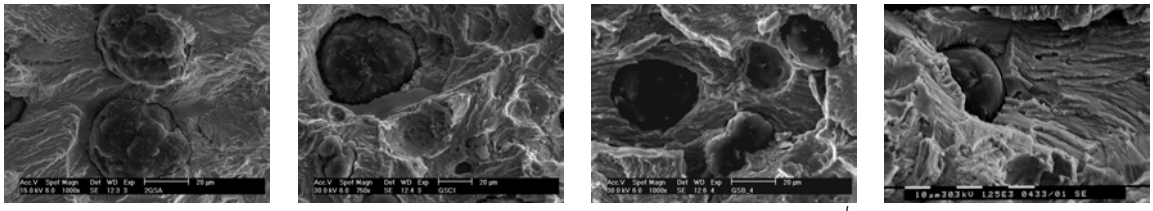

Figure 6: SEM fracture surface analysis (R = 0.5, ΔK = 10 MPa√m). From left to right: ferritic, ferrito-pearlitic, pearlitic and austempered ductile iron. Crack growth from left to right.

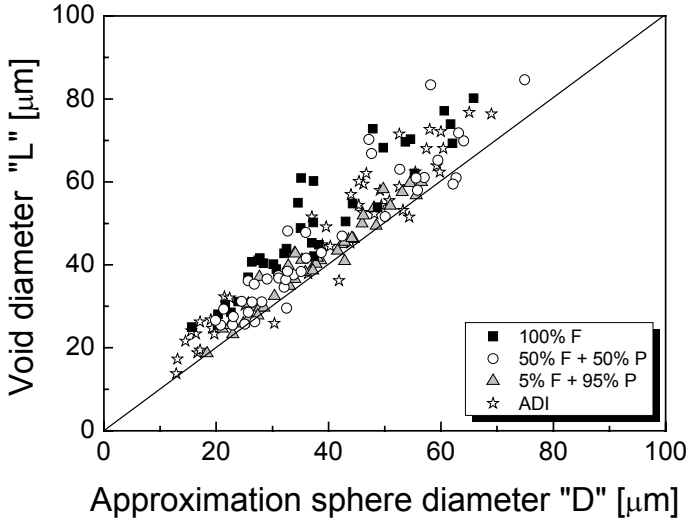

Figure 7: Four investigated ductile irons. Approximation sphere diameter – void diameter.

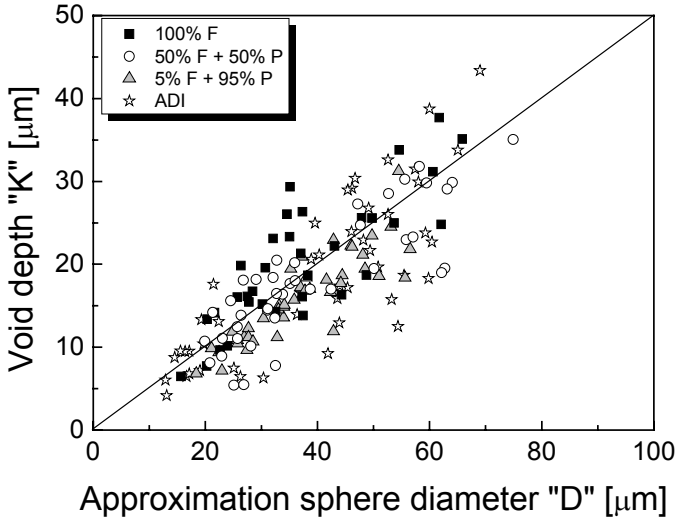

Figure 8: Four investigated ductile irons. Approximation sphere diameter – void depth.

Almost all the investigated voids are characterized by "L > D", for all the investigated microstructures. It implies that a ductile component in the debonding mechanism is always present. Microstructure strongly affects the experimental results distribution. Pearlitic ductile iron is characterized by the lowest differences "L - D" (completely fragile debonding corresponds to "L – D = 0"), and fully ferritic ductile iron is characterized by the higher "L-D" values (higher ductile deformation during debonding).

Ferritic-pearlitic ductile iron shows intermediate "L-D" values. This is probably due to the different mechanical behaviour of ferritic shields and pearlitic matrix that induces a compression stress state in ferritic shields corresponding to K_{min}, with a consequent increase of the importance of plasticity induced crack closure effect and a decrease of the crack growth rate. Graphite spheroids ductile debonding appears to be reduced, if compared to ferritic ductile iron (lower "L-D" values).

Austempered ductile iron is characterized by "L-D" experimental results distribution that is similar to ferritic-pearlitic ductile iron and probably crack closure mechanisms are the same as in ferritic-pearlitic ductile iron, due to the presence of residual ferrite around graphite elements. Differences in the mechanical behaviour of pearlite and bainite are not so relevant. In fact, ferritic-pearlitic and austempered ductile irons crack growth rates are comparable for all the investigated experimental conditions (Fig. 5). Microstructure and fracture surface analysis of austempered ductile iron shows that it is still possible an increase of the crack propagation resistance by means of an increase of the microstructure control, controlling both the residual ferrite volume fraction and the graphite elements degeneration.

Also the analysis of voids depths "K" as a function of the approximation sphere diameters "D" allows to obtain an analogous classification of the importance of the ductile deformation in the debonding mechanism, with the fully pearlitic microstructure that is characterized by "$K \leq D/2$" (completely fragile spheroids debonding) and other investigated microstructures that are characterized by a higher importance of the ductile deformation in the debonding mechanism, with a consequent higher scatter of the experimental results.

Quantitative analysis shows the importance of two different crack closure mechanisms in ductile irons fatigue crack propagation. Considering monophasic ductile irons, graphite elements ductile debonding is the main crack closure mechanism, and higher ductile deformation corresponds to the lower crack growth rates. Two phases ductile irons are also characterized by a plasticity induced crack closure effect due to the different mechanical behaviour of ferrite-pearlite or ferrite-bainite and to the peculiar phases distribution (ferritic shields around graphite elements). As a consequence, a reduction of the importance of graphite elements ductile debonding is obtained, but crack growth rates are lower than monophasic ductile irons.

CONCLUSIONS

Experimental results allow to summarize the following considerations:

- microstructure influences ductile irons fatigue crack propagation resistance only considering high R values; lower R values correspond to the same crack growth rates;
- SEM fracture surface analysis allowed to quantify the importance of graphite elements ductile debonding as a crack closure mechanism for monophasic ductile irons;
- Ferritic-pearlitic and austempered ductile irons are characterized by a peculiar phases distribution (ferritic shields around graphite elements) and this implies an increase of the importance of plasticity induced crack closure effect and a reduction of the importance of graphite elements ductile debonding.

Austempered ductile iron fatigue crack propagation resistance could be improved by means both an optimization of the residual ferrite volume fraction and a reduction of graphite elements degeneration.

REFERENCES

1. Ward, R.G. (1962), *An introduction to the physical chemistry of iron and steel making,* Arnold, London.
2. Labrecque, C. Gagne, M. (1998) *Canadian Metallurgical Quarterly*, **37**, 5, 343-378.
3. Tokaji, K. Ogawa, T. and Shamoto, K. (1994), *Fatigue*, **16**, 344-350.
4. Iacoviello, F. Di Cocco, V. (2003) *International Conference on Fatigue Crack Paths*, Parma (Italy), n. 116.
5. *ASTM Standard test Method for Measurements of fatigue crack growth rates (E647-93)*, Annual Book of ASTM Standards, (1993), 0301, American Society for Testing and Materials.
6. Iacoviello, F. Di Bartolomeo, O. and Cavallini, M. (2004) *AIM National Conference*, Vicenza (Italy), n. 19,.
7. Iacoviello, F. Cavallini, M. (2003) *La Metallurgia Italiana,* **1**, 31-37.